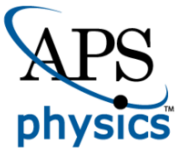

Two-Photon X-Ray Diffraction

J. Stöhr

Phys. Rev. Lett. **118**, 024801 — Published 11 January 2017

DOI: 10.1103/PhysRevLett.118.024801

Two-Photon X-Ray Diffraction

J. Stöhr*
SLAC National Accelerator Laboratory and Department of Photon Science, Stanford, California 94035, USA

The interference pattern of a circular photon source has long been used to define the optical diffraction limit. Here we show the breakdown of conventional x-ray diffraction theory for the fundamental case of a "source", consisting of a back-illuminated thin film in a circular aperture. When the conventional spontaneous x-ray scattering by atoms in the film is replaced at high incident intensity by stimulated resonant scattering, the film becomes the source of cloned photon twins and the diffraction pattern becomes self-focussed beyond the diffraction limit. The case of cloned photon pairs is compared to and distinguished from entangled photon pairs or biphotons.

The fundamental interactions of x-rays with matter, absorption, emission and scattering have historically been treated in two different pictures. While x-ray absorption and emission are viewed quantum mechanically in a photon-based picture as the irreversible transfer of energy between photons and electrons, elastic x-ray scattering and diffraction are treated classically in terms of electromagnetic waves. The success of the classical treatment of x-ray scattering and diffraction can be explained by Dirac's premise that diffraction occurs one-photon-at-a-time [1], with the classical treatment simply expressing the single photon field as a wave. This treatment has served us well for the first one hundred years of x-ray science since even for the brightest synchrotron radiation sources, on average, less than a single photon was present in a typical sample volume [2]. With the advent of x-ray free electron lasers (XFELs) [3], conventional diffraction theory has to be revisited due to the simultaneous presence of many indistinguishable (coherent) photons corresponding to a photon degeneracy parameter $n_{\rm coh} \gg 1$. Fig. 1 shows the historical evolution of x-ray source brightness, with the peak brightness $\mathcal{B}_{\rm peak}$ directly linked to the photon degeneracy parameter according to [4],

$$n_{\rm coh} = \frac{\mathcal{B}_{\rm peak}\lambda^3}{8\,c} \qquad (1)$$

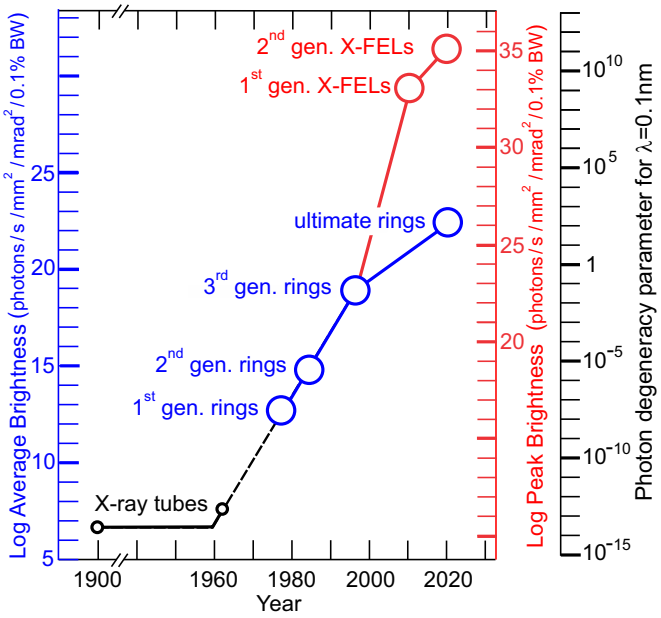

FIG. 1: Historical and projected future increase in average brightness of storage rings (blue) and peak brightness of XFELs (red). On the right we have also given in black the number of photons per coherence volume or degeneracy parameter, calculated from the peak brightness with (1) for a wavelength of $\lambda = 0.1\,$nm. In practice, the achievable degeneracy parameter is lowered by beam line losses

Here we address one of the most fundamental and important diffraction problems, the interference pattern of a circular quasi-monochromatic source. This case is also encountered in coherent x-ray imaging experiments [5, 6], where a thin film in a coherently illuminated circular aperture represents the "source". When the intensity distribution is uniform (flat-top) across the circular source area, the diffraction pattern is the well known Airy pattern and the width of the central intensity peak defines the fundamental diffraction limit.

We show the breakdown of conventional diffraction theory at high incident intensities, when spontaneous scattering is replaced by stimulated scattering in a film source, leading to complete x-ray transparency [7, 8]. One would then expect that the stimulated Airy diffraction pattern is that of the aperture without the film. We show that this is not the case. Instead, the stimulated pattern becomes the square of the Airy pattern, with a reduction of the diffraction-limited width of the central peak and the effective disappearance of the outer Airy rings. The new diffraction pattern arises from the cooperative interaction of two coherent photons in a resonant scattering process. The cloned photon pairs, created by impulsive stimulated emission, propagate together in the forward direction.

Stimulation or cloning [9, 10] in the sample itself, discussed here, is shown to be related to the diffraction of *entangled* photon pairs or biphotons [11, 12], which are incident on the sample from a parametric down conversion source [13–17]. While biphoton diffraction doubles the spatial frequency [13, 16], cloned photon pairs are

shown to lead to a squared intensity of the one-photon pattern.

For the calculation of two-photon diffraction, we assume that the fields incident on the circular aperture of area $A_s = \pi R^2$ are *longitudinally coherent* in the sense that the coherence length $\ell_{coh} = \lambda^2/\Delta\lambda$ is much larger than the film thickness d. This allows us to treat the film response in terms of a two-dimensional sheet with atomic area density $N_a/A_s = \rho_a d$, where ρ_a is the atomic volume density. In the derivation of the diffraction pattern we follow Fig. 2.

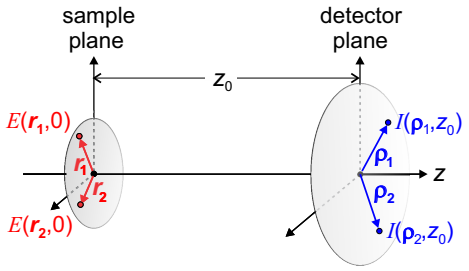

FIG. 2: Assumed diffraction geometry. The incident fields $E(\boldsymbol{r}_1, 0)$ and $E(\boldsymbol{r}_2, 0)$ in the sample plane constitute a two-photon amplitude. The diffracted intensities $I(\boldsymbol{\rho}_1, z_0)$ and $I(\boldsymbol{\rho}_2, z_0)$ are observed in coincidence in the distant detector plane.

For our discussion and distinction of one- and two-photon diffraction, we associate a real field with each individual photon according to,

$$\begin{aligned} \boldsymbol{E}(\boldsymbol{r}, t) &= \boldsymbol{E}_0 \left[e^{\mathrm{i}(\boldsymbol{k}\cdot\boldsymbol{r} - \omega t)} + e^{-\mathrm{i}(\boldsymbol{k}\cdot\boldsymbol{r} - \omega t)} \right] \\ &= 2\boldsymbol{E}_0 \cos(\boldsymbol{k}\cdot\boldsymbol{r} - \omega t) \end{aligned} \tag{2}$$

where the field amplitude of a single photon in wavevector mode k is given by the quantized field expression,

$$E_0 = \sqrt{\frac{\hbar\omega_k}{2\epsilon_0 V_k}}, \qquad V_k = \frac{8\pi^3}{k^2 \Delta k} \tag{3}$$

The number of photons of a given polarization in the coherence or mode volume V_k is the photon degeneracy parameter plotted in Fig. 1. The incident intensity per photon is given by a two-field correlation function whose time average is given by,

$$I_0 = \epsilon_0 c \langle E^2(\boldsymbol{r}, t) \rangle = 4\epsilon_0 c E_0 \langle \cos^2(\boldsymbol{k}\cdot\boldsymbol{r} - \omega t) \rangle = 2\epsilon_0 c E_0^2 \tag{4}$$

where ϵ_0 the dielectric constant of the vacuum and c is the speed of light. The total incident intensity of a beam of n_0 photons is then given by $n_0 I_0$.

Below we treat the diffraction of photons by an aperture which may contain a thin film, assumed to be non-magnetic and of uniform charge distribution without orientational order. The atomic resonant scattering is then independent of polarization and simply determined by the atomic charge. We distinguish the conventional one-photon-at-a-time diffraction pattern from the pattern where two coherent photons are simultaneously present in the sample plane at $z = 0$. We describe the two-photon probability amplitude in the sample plane as [16],

$$F(\boldsymbol{r}_1, \boldsymbol{r}_2) = E(\boldsymbol{r}_1, 0) E(\boldsymbol{r}_2, 0)\, g(\boldsymbol{r}_1, \boldsymbol{r}_2) \tag{5}$$

The function $g(\boldsymbol{r}_1, \boldsymbol{r}_2)$ characterizes the spatial correlation between the single photon fields at lateral points $\boldsymbol{r}_1$ and $\boldsymbol{r}_2$, as shown in Fig. 2.

The diffraction pattern in a distant detector plane originating from a coherently illuminated sample (see Fig. 2) is typically calculated in a classical picture based on the interference of electromagnetic waves (EM) by use of the Rayleigh-Sommerfeld diffraction formula in the Fraunhofer approximation [18]. Since interference occurs by a single photon field with itself, the diffracted intensity is then related to the one-photon field (2) at a point $(\boldsymbol{\rho}, z_0)$ in the detector plane by,

$$I^{(1)}(\boldsymbol{\rho}, z_0) = 2\epsilon_0 c E^2(\boldsymbol{\rho}, z_0) \tag{6}$$

where the superscript indicates the one-photon nature. If all n_0 incident photons are coherent they produce the same pattern and the diffraction pattern is given by $n_0 I^{(1)}$. The granular diffraction pattern consists of single photon counts per pixel, which is statistically filled-in with increasing number n_0, as beautifully demonstrated by diffraction experiments with single electrons [19]. If the incident photons are laterally incoherent, the single-photon diffraction patterns, which add on an intensity basis, average to a broad incoherent intensity distribution in the detector plane. Remarkably, the Van-Cittert-Zernike theorem [20] can pick-out the coherent part of the intensity through the coincident detection of photons at two separate points in the detector plane.

In contrast to the one-photon coherent case, the diffracted two-photon intensity is defined through a four-field or two-intensity correlation function as [15],

$$I^{(2)}(\boldsymbol{\rho}_1, \boldsymbol{\rho}_2, z_0) = \epsilon_0^2 c^2 \left\langle E_1^2(\boldsymbol{\rho}_1, z_0)\, E_2^2(\boldsymbol{\rho}_2, z_0) \right\rangle \tag{7}$$

In the Fraunhofer approximation, the diffracted two-photon intensity is given by [15, 16]

$$\begin{aligned} I^{(2)}(\boldsymbol{\rho}_1, \boldsymbol{\rho}_2, z_0) = \frac{\epsilon_0^2\, c^2\, C^2}{\lambda^4 z_0^4} \Bigg| \iiiint_{-\infty}^{\infty} E(\boldsymbol{r}_1, 0) E(\boldsymbol{r}_2, 0)\, g(\boldsymbol{r}_1, \boldsymbol{r}_2) \\ \times \exp\left[-\mathrm{i}\frac{2\pi}{\lambda z_0} (\boldsymbol{r}_1\cdot\boldsymbol{\rho}_1 + \boldsymbol{r}_2\cdot\boldsymbol{\rho}_2) \right] \mathrm{d}\boldsymbol{r}_1\, \mathrm{d}\boldsymbol{r}_2 \Bigg|^2 \end{aligned} \tag{8}$$

The constant C is determined by considering power conservation. For a transparent uniformly illuminated aperture of size A_s, for example, the incident power $I_0 A_s$ has to be equal to the total diffracted power in the detector plane so that,

$$\frac{1}{2} \iint_{-\infty}^{\infty} I^{(2)}(\boldsymbol{\rho}, z_0)\, \mathrm{d}\boldsymbol{\rho} = I_0 A_s \tag{9}$$

where the factor $1/2$ accounts for the two-photons in $I^{(2)}$. With time, the diffraction pattern will form through the addition of $n_0/2$ two-photon diffraction patterns.

The two-photon formalism can be used to describe stimulated diffraction by a film in an aperture. While diffraction by a hole alone or spontaneous diffraction by a film in a hole, can be described by spherical wave emission from each point or atom in the aperture plane, the famous Huygens-Fresnel principle, this description breaks down for stimulated atomic scattering. In this case, the atoms in the film no longer spontaneously scatter photons into random directions, which on average is well modeled by the Huygens-Fresnel spherical waves. Rather, the stimulating (idler) photons imprint their incident wavevector direction (mode) on the photon created in the stimulated decay. At saturation stimulation, the film becomes transparent [7, 8].

The limit of complete stimulation is described by (8) with $\boldsymbol{\rho}_1 = \boldsymbol{\rho}_2 = \boldsymbol{\rho}$ and $g(\boldsymbol{r}_1, \boldsymbol{r}_2) = 1$, meaning that the two-photon amplitude given by (5) is separable into individual photon contributions which are coherent but quantum mechanically unentangled. The integrals in (8) can then be independently evaluated to give,

$$I^{(2)}(\boldsymbol{\rho}, z_0) = \frac{\epsilon_0^2\, c^2\, C^2}{\lambda^4 z_0^4} \left| \iint_{-\infty}^{\infty} E(\boldsymbol{r}) \exp\left[-\mathrm{i}\frac{2\pi}{\lambda z_0}\boldsymbol{r}\cdot\boldsymbol{\rho}\right] \mathrm{d}\boldsymbol{r} \right|^4 \quad (10)$$

If the two intensities in (7) are temporally uncorrelated, we have $I^{(1)} = \sqrt{I^{(2)}}$ and with $C = 1$ we recover from (10) the one-photon Fraunhofer diffraction formula.

For the case of a circular aperture of area $A_\mathrm{s} = \pi R^2$, the field of each incident photon is uniform and given by

$$E(\boldsymbol{r}, 0) = \begin{cases} E_0 & -R < r < +R \\ 0 & \text{otherwise} \end{cases} \quad (11)$$

In this case the diffracted one-photon intensity takes the form of the Airy pattern, which as a function of momentum transfer $q = k\rho/z_0$ is given by [18],

$$I^{(1)}(q, z_0) = I_0 \frac{A_\mathrm{s}^2}{\lambda^2 z_0^2} \left[\frac{2J_1(qR)}{qR}\right]^2 \quad (12)$$

The corresponding spontaneous diffraction pattern in the presence of the film is simply the Airy pattern of the hole, attenuated according to the Beer-Lambert law,

$$I_\mathrm{spon} = I^{(1)}(q, z_0)\, \mathrm{e}^{-2\beta_0 k d} \quad (13)$$

where β_0 is the optical absorption constant [7, 21].

The two-photon intensity for the case of saturation stimulation is naturally coincident and consists of two-photon events at all points in the detector plane. By evaluating (7) as $I^{(2)} = 4\epsilon_0^2 c^2 E^4$ and determining C in (10) with (9), we obtain,

$$I_\mathrm{stim} = I^{(2)}(q, z_0) = I_0 \frac{1}{1 - 16/(3\pi^2)} \frac{A_\mathrm{s}^2}{\lambda^2 z_0^2} \left[\frac{2J_1(qR)}{qR}\right]^4 \quad (14)$$

The two-photon coincidence pattern differs from the one-photon pattern through the power conserving prefactor $1/(1 - 16/(3\pi^2)) = 2.17$ and, most importantly, it is the *squared* one-photon Airy distribution. The power in the detector plane, given by the area integrals of $I^{(1)}$ and $I^{(2)}$, is the same.

Fig. 3 compares the diffraction patterns for a circular aperture for the parameters of the experiment reported in Ref. [8], $\lambda = 1.6\,\mathrm{nm}$ (Co L_3 resonance) and a circular aperture hole of $R = 725\,\mathrm{nm}$. The intensity is plotted as a function of momentum transfer q/q_0, where $q_0 = 1.22\pi/R$ is the first node of the Airy pattern. The conventional Airy pattern of the hole, given by (12) and shown as a black curve, contains 83.8% of the power in the central disc. The stimulated pattern, given by (14) and shown in red, contains 99.8% of the power in the central disk, so that the outer Airy rings have negligible intensity. The spontaneous Airy pattern given by (13) is shown in blue, assuming the presence of a $d = 20\,\mathrm{nm}$ thick Co film with optical constant $\beta_0 = 0.0075$. In this case the power is reduced by a factor of $\simeq 3$ through absorption in the film. Fig. 3 (b) reveals the narrowing of the central Airy disc from the full width half maximum (FWHM) value $0.844\,q_0$ for the hole (black) and spontaneous film (blue) patterns, to $0.606\,q_0$ for the stimulated film (red).

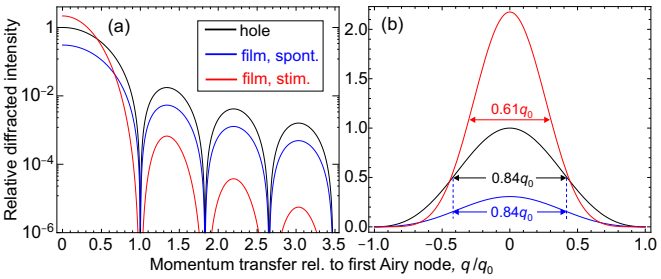

FIG. 3: (a) Airy diffraction intensity as a function of normalized momentum transfer q/q_0, where $q_0 = 1.22\pi/R$ is the first node of the Airy pattern. We have assumed $\lambda = 1.6\,\mathrm{nm}$ (Co L_3 resonance) and a circular hole of radius $R = 725\,\mathrm{nm}$ in an aperture. The pattern of the hole (black) is given by (12), the spontaneous diffraction pattern for an inserted 20 nm thick Co film (blue) is given by (13), and the stimulated two-photon diffraction pattern (red) is given by (14). (b) Enlarged pattern around the optical axis ($q = 0$), revealing the reduction of the width of the stimulated pattern.

Our above discussion was restricted to the case of complete (saturation) stimulation. In order to derive the evolution with incident intensity from the blue spontaneous pattern in Fig. 3 to the red stimulated pattern, we describe the response of the film in terms of the spontaneous, β_0, and non-linear, β_NL, optical parameters as done in Ref. [8]. The pattern in the presence of spontaneous and stimulated scattering is obtained by considering that the total diffracted power in the detector plane has to be equal to the transmitted power in the exit plane of the sample. The total intensity-dependent diffraction

pattern is obtained as,

$$I_{\rm tot}(q,z_0) \;=\; \frac{1-{\rm e}^{-2(\beta_0+\beta_{\rm NL})kd}}{1-{\rm e}^{-2\beta_0 kd}}\, I_{\rm spon}(q,z_0) + \frac{{\rm e}^{-2\beta_{\rm NL}kd}-1}{{\rm e}^{2\beta_0 kd}-1}\, I_{\rm stim}(q,z_0) \qquad (15)$$

with $I_{\rm spon}$ given by (13) and $I_{\rm stim}$ by (14).

In Fig. 4 we plot the change in the Airy diffraction pattern with increasing x-ray intensity for the example of a 20 nm thick Co film in a circular aperture, calculated with (15) and use of the optical parameters of Refs. [7, 8].

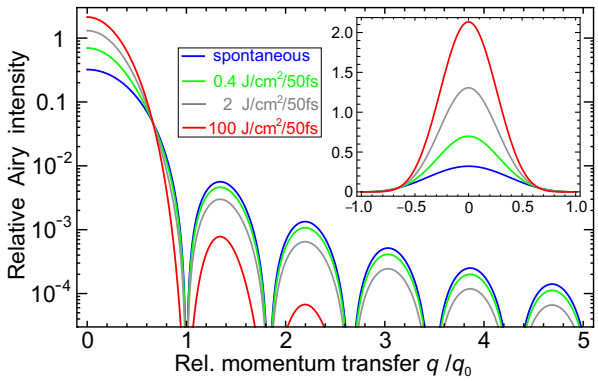

FIG. 4: Airy diffraction pattern, intensity versus momentum transfer, calculated with (15) for a circular hole of area $A_{\rm s} = \pi R^2$ with $R = 725$ nm containing a 20 nm thick Co film and assuming Co L_3 ($\lambda = 1.6$ nm) resonant excitation. The blue curve is the same as in Fig. 3, and the other curves are for different intensities of a 50 fs SASE pulse consisting of two 20 fs coherent sub-pulses. The momentum transfer is scaled relative to the first node of the Airy pattern at $q_0 = 1.22\pi/R$. The inset shows the enlarged pattern around the optical axis ($q=0$), revealing the intensity change in the central Airy disk.

For the calculation of $\beta_{\rm NL}$, which depends both on the incident intensity I_0 and the sample thickness d, we included the change of the intensity through the 20 nm Co film, which is approximately given by the analytical expression in [8] with the replacement of I_0 by $I_0/2$.

In Fig. 5 we have plotted as a thick gray curve the intensity-dependent contrast of the outer Airy rings given by,

$$\frac{I_{\rm tot}(q\gg q_0,z_0)}{I_{\rm spon}(q\gg q_0,z_0)} = \frac{1-{\rm e}^{-2(\beta_0+\beta_{\rm NL})kd}}{1-{\rm e}^{-2\beta_0 kd}}. \qquad (16)$$

There is excellent agreement with the available experimental data points (red circles) of Ref. [8], extending to $I_0 \le 340\,{\rm mJ/cm^2/50\,fs}$. Higher intensities could be achieved by reducing the focus spot size below the used value of 10 μm.

Our complete description of the change of the Airy pattern in the presence of stimulation overcomes the unsatisfactory *ad hoc* division of the pattern into regions $q > q_0$ and $q < q_0$ assumed in Ref. [8]. In particular,

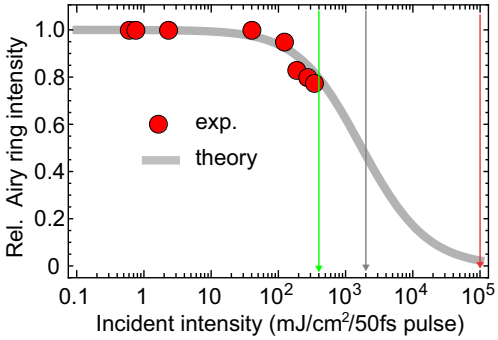

FIG. 5: Comparison of the observed Airy diffraction contrast relative to spontaneous contrast (red circles) as a function of incident intensity for monochromatized 50 fs SASE pulses [8] and calculated change (thick gray line) upon stimulation using (15). The vertical lines indicate the three intensity values used in Fig. 4.

we find that the stimulated pattern corresponds to the squared one-photon pattern, which effectively eliminates out-of-beam diffraction at the expense of intensity pile up in the forward direction around $q=0$.

The case of biphoton diffraction by an aperture alone is also described by (8). The entanglement of the biphotons used to illuminate the diffracting aperture is generated in the parametric down conversion source and may be represented by $g(\boldsymbol{r}_1,\boldsymbol{r}_2)=\delta(\boldsymbol{r}_1-\boldsymbol{r}_2)$ in the aperture plane [16]. In the momentum transfer notation $\boldsymbol{q} = k\boldsymbol{\rho}/z_0$, the two-photon coincidence intensity given by (8) with $\boldsymbol{\rho}_1=\boldsymbol{\rho}_2$ becomes,

$$I^{(2)}(\boldsymbol{q},z_0)=\frac{\epsilon_0^2\,c^2\,C^2}{\lambda^4 z_0^4}\left|\iint_{-\infty}^{\infty}|E(\boldsymbol{r},0)|^2\,\exp[-{\rm i}\,\boldsymbol{r}\cdot(\boldsymbol{q}+\boldsymbol{q})]{\rm d}\boldsymbol{r}\right|^2 \qquad (17)$$

This is the biphoton version of the van Cittert–Zernike theorem [15]. Now the total momentum transfer $\boldsymbol{Q}=\boldsymbol{q}+\boldsymbol{q}$ that determines the diffracted intensity corresponds to that of the original beam that generated the two parametric down converted photons.

For a given field distribution $E(\boldsymbol{r},0)$, the constant C is again determined by requiring power conservation according to (9), and for a circular aperture, (17) is evaluated as,

$$I^{(2)}(\rho,z_0)=2I_0\,\frac{A_{\rm s}^2}{\lambda^2 z_0^2}\left[\frac{2J_1(2qR)}{2qR}\right]^2 \qquad (18)$$

The diffraction patterns thus corresponds to $Q=2q$ or a wavelength of $\lambda/2$ as observed experimentally in the optical regime [13, 16]. For the circular hole case, the pattern has twice the periodicity in the detector plane as illustrated by the green curve in Fig. 6 (a).

In particular, the width of the central Airy disk is reduced by a factor of two as illustrated in Fig. 6 (b). Since this width defines the diffraction limit according to the

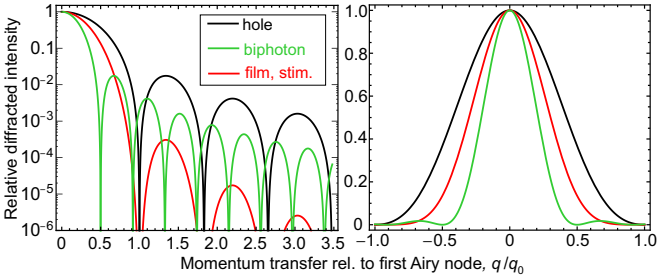

FIG. 6: (a) Airy diffraction intensity, scaled to unity at $q=0$ for better comparison, versus momentum transfer for a circular hole, using the same parameters as for Fig. 3. We compare the one-photon (black) and biphoton (green) hole patterns to the stimulated Co film (red) pattern. (b) Enlarged distribution around the optical axis. The hole pattern has a FWHM $0.844\,q_0$ (black), the stimulated film pattern $0.606\,q_0$ (red) and the biphoton pattern $0.422\,q_0$ (green).

Rayleigh criterion, the use of biphotons or even multiphotons [12] has attracted much interest and called "quantum lithography" [14, 22]. Parametric down conversion has also been demonstrated in the x-ray regime [23, 24], and the increased brightness of XFELs now opens the door for diffraction experiments with x-ray biphotons.

In summary, we show that the conventional one-photon-at-a-time diffraction pattern of a thin film in an aperture is changed through impulsive stimulation by the incident beam. The stimulated intensity pattern, created by cloned photon pairs, is the square of the one-photon pattern and is self-focussed beyond the diffraction limit. The increased concentration in the forward direction leads to a loss of out-of-beam diffraction.

This work was supported by the U.S. Department of Energy, Office of Basic Energy Sciences under Contract No. DE-AC02- 76SF00515. I would like to thank D. J. Higley for triggering this study and J. W. Goodman and E. L. Saldin for valuable discussions.

* Electronic address: stohr@stanford.edu

[1] P. A. M. Dirac, *Quantum Mechanics, 4th ed.*, (Oxford University Press, 1958), page 9.
[2] B. Lengeler, Naturwissenschaften **88**, 249 (2001).
[3] C. Bostedt et al., Rev. Mod. Phys. **88**, 015007 (2016).
[4] This expression holds for a spatially and temporally coherent Gaussian pulse. It differs by a factor $\sqrt{2}$ from that for a temporally incoherent Gaussian pulse, given by Eq. (19) in E. L. Saldin, E. A. Schneidmiller, and M. V. Yurkov, Opt. Commun. 281, 1179 (2007).
[5] S. Eisebitt et al., Nature (London) **432**, 885, (2004).
[6] T. Wang et al., Phys. Rev. Lett., **108**, 267403 (2012).
[7] J. Stöhr and A. Scherz, Phys. Rev. Lett. **115**, 107402 (2015); *ibid* **116**, 019902 (2016).
[8] B. Wu et al., Phys. Rev. Lett. **117**, 027401 (2016).
[9] C. Simon, G. Weihs and A. Zeilinger, Phys. Rev. Lett. **84**, 2993 (2000).
[10] A. Lamas-Linares, C. Simon, J. C. Howell and D. Bouwmeester, Science **296**, 712 (2002).
[11] D. N. Klyshko, *Photons and Nonlinear Optics*, (Gordon and Breach, New York, 1988).
[12] J. Jacobson, G. Bjork, I. Chuang, and Y. Yamamoto, Phys. Rev. Lett. **74**, 4835 (1995).
[13] E. J. S. Fonseca, C. H. Monken, and S. Pádua, Phys. Rev. Lett. **82**, 2868 (1999).
[14] A. N. Boto, P. Kok, D. S. Abrams, S. L. Braunstein, C. P. Williams, and J. P. Dowling, Phys. Rev. Lett., **85** , 2733 (2000).
[15] B. E. A. Saleh, A. F. Abouraddy, A. V. Sergienko, and M. C. Teich, Phys. Rev. A **62**, 043816 (2000).
[16] K. Edamatsu, R. Shimizu, and T. Itoh, Phys. Rev. Lett. **89**, 213601 (2002); R. Shimizu and K. Edamatsu and T. Itoh, Phys. Rev. A **67**, 041805 (2003); *ibid* **74**, 013801 (2006).
[17] For reviews see: M. DAngelo and Y.H. Shih, Laser Phys. Lett. **2**, 567 (2005); A. Zeilinger, G. Weihs, T. Jennewein and M. Aspelmeyer, Nature (London) **433**, 230 (2005).
[18] J. W. Goodman, *Introduction to Fourier Optics, Third edition*, (Roberts and Co., 2005).
[19] R. Bach, D. Pope, Sy-Hwang Liou and H. Batelaan, New J. Phys. **15**, 033018 (2013).
[20] J. W. Goodman, *Statistical Optics, Second edition*, (Wiley, 2015).
[21] J. Stöhr and H. C. Siegmann, *Magnetism: From Fundamentals to Nanoscale Dynamics*, (Springer, Heidelberg, 2006).
[22] M. DAngelo, M. V. Chekhova, and Y. Shih, Phys. Rev. Lett., **87** 013602 (2001).
[23] K. Tamasaku, K. Sawada, E. Nishibori, and T. Ishikawa, Nature Phys. (London) **7**, 705 (2011).
[24] S. Shwartz et al., Phys. Rev. Lett. **109**, 013602 (2012).